Case Studies in Chemical and Environmental Engineering 9 (2024) 100642

Contents lists available at ScienceDirect

Case Studies in Chemical and Environmental Engineering

journal homepage: www.sciencedirect.com/journal/case-studies-in-chemical-and-environmental-engineering

Case Report

Effects of sodium alginate-poly(acrylic acid) cross-linked hydrogel beads on soil conditioner in the absence and presence of phosphate and carbonate ions

Endar Hidayat [a,b,c,*], Nur Maisarah Mohamad Sarbani [a,b], Sudip Kumar Lahiri [d,e], Sadaki Samitsu [c], Seiichiro Yonemura [a,b], Yoshiharu Mitoma [a,b], Hiroyuki Harada [a,b]

[a] Graduate School of Comprehensive Scientific Research, Program in Biological System Sciences, Prefectural University of Hiroshima, Shobara, 727-0023, Japan
[b] Department of Life System Science, Faculty of Bioresources Science, Prefectural University of Hiroshima, Shobara, 727-0023, Japan
[c] Data-driven Polymer Design Group, Research Center for Macromolecules and Biomaterials, National Institute for Materials Science, 1−2−1 Sengen, Tsukuba, 305-0047, Japan
[d] Department of Mechanical & Industrial Engineering, University of Toronto, Toronto, Ontario, M5S 3G8, Canada
[e] Faculty of Allied Health Sciences, Chettinad Hospital and Research Institute, Chettinad Academy of Research and Education, Kelambakkam, 603103, Tamil Nadu, India

ARTICLE INFO

Keywords:
Hydrogel beads
Sodium alginate
Poly (acrylic acid)
Soil water retention
Swelling
Soil characteristics
Anionic ions

ABSTRACT

Hydrogel beads, composed of polymers, possess the ability to absorb substantial quantities of water simultaneously and gradually release it in dry conditions. In this work, hydrogel beads were synthesized using sodium alginate (S-Alg) and poly (acrylic acid) (P-Acc), either in the absence or presence of phosphate (PO_4^{3-}) (S-Alg/P-Acc@PO_4^{3-}) and carbonate (CO_3^{2-}) anionic ions (S-Alg/P-Acc@CO_3^{2-}). Subsequently, these beads were cross-linked with Ca^{2+} ions. The scanning electron microscopy (SEM) images demonstrated that the presence of anionic ions has an impact on the structure of the hydrogel beads and enhances porosity expansion while concurrently reducing the concentration of carboxyl (COOH) groups. The hydrogel beads exhibited a great swelling behavior, with S-Alg/P-Acc@CO_3^{2-} capable of absorbing up to 73.5 % of water in acidic conditions, but decreased under neutral and basic conditions. Soil water loss (SWL) experiments confirmed the ability of hydrogel beads to retain water in the soil. Additionally, observations of soil characteristics after a 14-day treatment revealed no significant difference in pH and C/N ratio (P-value <0.05). However, soil's available Fe and N–NO_3^- significantly reduced (P-value <0.05) while substantially promoting soil N–NH_4^+, available phosphorus (P), cation exchange capacity (CEC), soil organic carbon (SOC), and exchangeable cation (Ca^{2+}, K^+ and Mg^{2+}). The presence of hydroxyl (-OH) and –COOH groups was found to be crucial for enhancing soil properties.

1. Introduction

The global agricultural landscape confronts significant challenges arising from the increase in global population and the growing impact of climate change. This has resulted in a rising need for innovative approaches to tackle the interconnected problems of water scarcity and soil degradation [1]. The productivity of agricultural food production is heavily dependent on soil quality and the availability of sufficient water. Human activities, such as unsustainable agricultural practices, deforestation, and soil pollution, can lead to soil mismanagement, erosion, and diminishing fertile land, which may negatively impact the production of food [2]. Inadequate rainfall and ineffective utilization of accessible water substantially affect the quantity and quality of food produced. Consequently, crop productivity is declining annually, endangering the global food security. To ensure sufficient availability of food, it is crucial to rehabilitate deteriorating soils and optimize the utilization of limited natural resources, such as rainfall. A key research challenge involves devising innovative solutions to overcome existing limitations and enhance soil quality and yield to meet global demands [3,4]. In this context, hydrogels have emerged as a revolutionary technology with the potential to address the aforementioned issues, as evidenced by recent advancements in materials science.

Hydrogels are hydrophilic polymer material networks cross-linked in three-dimensional (3D) structures consisting of physical, chemical, or

* Corresponding author. Graduate School of Comprehensive Scientific Research, Program in Biological System Sciences, Prefectural University of Hiroshima, Shobara, 727-0023, Japan.
E-mail address: hidayatendar1@gmail.com (E. Hidayat).

https://doi.org/10.1016/j.cscee.2024.100642
Received 19 December 2023; Received in revised form 25 January 2024; Accepted 27 January 2024
Available online 29 January 2024

dual cross-links. In physical cross-linking, a reversible network is assembled by various non-covalent interactions such as electrostatic interactions, hydrogen bonding, hydrophobic interactions, and molecular entanglements [5]. In chemical cross-linking, a permanent network is formed by covalent bonds between polymer chains using reactive cross-linking agents, such as glutaraldehyde [6] and epichlorohydrin [7], or the formation of strong ionic bonds using polyanions such as sodium triphosphate, sodium oxalate, and sodium citrate [8]. Hydrogels have the ability to absorb a significant quantity of water inside their frameworks and act as hydration packs, taking in water through osmotic pressure caused by the hydration of the polymer chains [9–12]. Upon integration into the soil, they form a complex structure that increases air circulation, mitigates soil compression, and increases the capacity to retain nutrients. On the other hand, hydrogel beads offer a more controlled and targeted approach to water retention, as a way to enhance the fertility of the soil and stimulate the development of better root systems, which eventually resulting in more vigorous plant growth [13]. The use of hydrogel beads for soil conditioning has emerged as a promising technology for revitalizing degraded land and fostering sustainable agricultural practices.

Sodium alginate (S-Alg) is a non-toxic and environmentally degradable copolymer polysaccharide composed of linear chains of β-D-mannuronic acid and α-L-guluronic acid connected by (1−4) linkages. S-Alg is usually extracted from brown algae and has been used for extensive applications such as the controlled release of diclofenac sodium [14], arsenic reduction [15], removal of copper and lead [16], and dye adsorption [17]. The ionotropic gelation of S-Alg using divalent metal ions, namely Ca^{2+}, is a simple and efficient technique for creating spherical hydrogel beads. Meng et al. demonstrated that metal ions exhibit stronger attractive interactions with carboxylic group compared with other functional sites on polysaccharides [18]. This interaction may have promoted the gel formation of polysaccharides on the membrane surfaces. Another study reported that the presence of carboxylic groups in the soil may improve its properties and regulate the distribution and availability of micronutrients to plants [19]. Additionally, carboxylic groups can control the levels of organic carbon in the soil [20] and boost the biological activities within the soil [21]. Poly (acrylic acid) (P-Acc) polymer is well recognized for its functional carboxylic groups [22] and capacity to enhance the mechanical strength of hydrogels [23].

Phosphate (PO_4^{3-}) anions are one of the major macronutrients essential for crops to promote healthier root systems and to improve overall plant growth and stability. Carbonate (CO_3^{2-}) anions can contribute to soil aggregation, improve soil structure, facilitate water retention, and act as a soil buffer. Other than supplying mineral source, CO_3^{2-} may also improve the morphology, structural stability, and strength, as well as increase the porosity of the hydrogel beads [24]. The hydrogel bead structure with these anions allows for the absorption and slow release of water, contributing to consistent soil moisture levels for plant roots.

In this study, we synthesized S-Alg/P-Acc-cross-linked hydrogel beads with and without PO_4^{3-} and CO_3^{2-} anions. The hydrogel beads were characterized using scanning electron microscopy (SEM), Fourier transform infrared spectroscopy (FTIR), titration (carboxyl group), and porosity analysis. The swelling behavior, soil water retention, and soil characteristics were also examined. The hydrogel beads functioned as storage medium for water by absorbing and retaining water inside the polymer network. This can efficiently reduced irrigation and improved soil characteristics, which are potentially useful for soil reformulation.

2. Materials and method

2.1. Materials

Calcium chloride ($CaCl_2$, 99 %), hydrochloric acid (HCl, 36.5–38 %), sulfuric acid (H_2SO_4, 95 %), potassium chloride (KCl, 99.5 %), sodium carbonate (Na_2CO_3, >99.8 %), sodium hydrogen phosphate ($NaHPO_4$, >99.95 %), sodium bicarbonate ($NaHCO_3$, >99.5 %), ammonium acetate (CH_3COONH_4, >97 %), potassium dichromate ($K_2Cr_2O_7$, 99.5 %) and sodium hydroxide (NaOH, 99.99 %) were purchased from Kanto Chemical Co. Inc., Japan. Sodium alginate (S-Alg) was purchased from Wako Chemicals, Tokyo, Japan. Poly (acrylic acid) (P-Acc) (molecular weight: 100.000) was purchased from Scientific Polymer Products, INC., New York.

2.2. Preparation of hydrogel beads

Hydrogel beads were formed by combining 6 mL of 1 wt% S-Alg aqueous solution, 6 mL of 5 wt% P-Acc aqueous solution, 1 mL of 3 M NaOH, and 1 mL of distilled water (DW) for the base S-Alg/P-Acc. To create functionalized variants, S-Alg/P-Acc@PO_4^{3-} and S-Alg/P-Acc@CO_3^{2-}, 1 mL of 2000 mg/L PO_4^{3-} and 1 mL of 2000 mg/L CO_3^{2-} were added, respectively, in place of DW. The samples were placed in bottle flasks and shaken on a rotary shaker (Rotator RT-50) for 1 h at room temperature (25°–30 °C). Then, the solution was injected slowly using a 10 mL syringe, one drop at a time, into a pre-prepared 10 wt% $CaCl_2$ aqueous solution. Subsequently, the hydrogel beads were allowed to grow for 90 min to obtain the resultant hydrogel beads. The hydrogel beads were then washed with ethanol and DW, and then let to dry in an oven at 60 °C for 24 h.

2.3. Determination of the porosity

Porosity was measured using the water displacement technique, following a previous study [25]. The hydrogel beads (1g) were immersed in ethanol for 24 h to remove unreacted monomers and create pores. The weight of the hydrogel beads was then measured with an electronic balance, and the porosity was determined using the following Eq. (2).

$$V_s = V - \left(\frac{W_2 - W_1 - W_0}{\rho}\right) \tag{1}$$

$$\text{Porosity}\ (\%) = \frac{(W_s - W_d)/\rho}{V_s} \tag{2}$$

where V_s is the volume of the hydrogel beads (cm^3), V is the volume of the ethanol solution (mL), W_2 is the weighted sum of the empty beaker, ethanol, and hydrogel beads (g), W_1 is the weight of empty beaker (g), W_0 is the weight of dried beads (g). ρ is the density of ethanol (0.7892 g/cm^3). where W_d is the dry weight of the beads, and W_s is the weight of the beads filled with ethanol.

2.4. Carboxyl groups analysis

The carboxyl content inside the cross-linked hydrogel beads was measured using conductometric titration [26]. In brief, ~25 mg of dried hydrogel bead composite was mixed with a 20 mM NaCl solution (2.5 mL), and the mixture was agitated for 30 min to achieve a uniform distribution. Subsequently, HCl (100 mM) was gradually introduced into the mixture to reach a pH value of 3.0. The suspension was then incrementally adjusted using a 10 mM NaOH solution to attain a pH of 11.0. The content of carboxyl group in the crosslinked hydrogel beads was quantified using Eq. (3).

$$\text{COOH}\ (\text{mmol}/\text{g}) = \frac{V_{\text{NaOH}} \times M_{\text{NaOH}}}{W_d} \tag{3}$$

where COOH (mmol/g) is the carboxyl content of the cross-linked hydrogel beads. V_{NaOH} (mL) represents the volume of NaOH required to deprotonate COOH groups. M_{NaOH} (mol/L) represents the molarity of the NaOH. where W_d (g) is the weight of the initial dry hydrogel beads.

2.5. Swelling experiments

The swelling characteristics of the hydrogel beads and the influence of pH were assessed. In brief, dried hydrogel beads were immersed in a glass beaker containing 25 mL of aqueous solution at pH 4, 7, and 9, prepared from DW and adjusted with 0.01 M NaOH and HCl solutions. The experiments were conducted at 25 °C for 24 h and the swelling ratio was calculated using the following Eq. (4).

$$\mathrm{SR}\ (\%) = \frac{W_s\text{-}W_d}{W_d} \times 100 \tag{4}$$

where W_s is the weights of swollen hydrogels and W_d is the weights of dried hydrogels.

2.6. Determination of soil water loss (SWL)

We measured soil water loss (SWL) in the soil over a period of 14 days. Soils were purchased from a shop market in Shobara City. Initially, the soils were dried by placing in an oven at 60 °C for 48 h. Then, 100 g of dried soil is placed into plastic container and subsequently, the dried hydrogel beads (1 g) were added. The soil was then watered with 100 ml of DW and weighed (W_i). The containers were kept in the laboratory under ambient air and temperature conditions and were weighed for up to 14 days (W_t). The SWL was calculated using Eq. (5) [27]:

$$\mathrm{SWL}\ (\%) = \frac{W_i\text{-}W_t}{\text{Soil Weight (g)}} \times 100 \tag{5}$$

2.7. Characterization of hydrogel beads

The functional groups on the hydrogel beads were analyzed using a Thermo Scientific Nicolet iS10 FTIR instrument (Thermo Fisher Scientific Inc., Waltham, MA, USA). The morphology of the hydrogel beads was examined using a benchtop SEM Miniscope TM-4000PlusII (Hitachi-hitech, Tokyo, Japan).

2.8. Determination of soil properties

To determine the pH and electrical conductivity (EC) of the soil, laboratory equipments including pH and EC meters, were utilized. Before analyzing the pH and EC, the soil and water were mixed at a ratio of 1:5 (w/v) and shaken for 30 min [28]. The C/N ratio was determined using a Macro-Corder JM1000 CN autosampler (JMA 1000). The Olsen technique [29] was used to quantify the available phosphorus (P) using a 0.5 M $NaHCO_3$ solution. Soil samples (1 g) were mixed with 20 mL $NaHCO_3$ and shaken for 30 min. Exchangeable cations (Ca^{2+}, K^+ and Mg^{2+}) were assessed using the 1 N CH_3COONH_4 extraction method, after which 10 wt% NaCl was added to the soil to determine its cation exchange capacity (CEC) [30]. The soil available N-NH_4^+ and N-NO_3^- were extracted using 2 M KCl. One gram of soil sample was shaken for 2 h at room temperature [31]. Soil organic carbon (SOC) was determined using the Walkley and Black wet oxidation method. Soil samples (0.5 g) were placed in a 100 mL beaker. Then, 5 mL of 1 N $K_2Cr_2O_7$ (98.1 potassium dichromate + 900 mL distilled water + 100 mL H_2SO_4) was added, shaken for a while and then 7.5 mL H_2SO_4 was added, and the mixture was allowed to stand for 30 min. Subsequently, the solution was subjected to distilled water up to a volume of 100 mL. Then, it was allowed to stand overnight and measured using a UV–Vis Spectrophotometer (JASCO V-530) at $\lambda = 561$ nm. Glucose was used as the standard organic carbon source. To estimate exchangeable Fe, the soil was treated with 20 mM $CaCl_2$ at a 1:5 ratio. After 30 min of shaking, the mixture was centrifuged at 5000 rpm for 10 min before being filtered. The Fe content was determined by pack testing at Kyoritsu Chemical-Check Lab., Corp. Kanagawa, Japan, using the reduction and *o*-phenanthroline methods.

2.9. Statistical analysis

Data analyses were performed with MINITAB software (version 21.3.1). Mean values were subjected to one-way analysis of variance (ANOVA), and treatment comparisons were conducted using Tukey's test (P-value <0.05).

3. Results and discussion

3.1. Characteristics of hydrogel beads

Fig. 1 displays the photograph of the dried hydrogel beads and impact on the absence and presence of PO_4^{3-} and CO_3^{2-} ions on the surface morphology. Based on top surface view, the dried hydrogel beads exhibited a rough surface with angular components for all hydrogel bead samples. The surface of hydrogel beads S-Alg/P-Acc@PO_4^{3-} (Fig. 1c2) and S-Alg/P-Acc@CO_3^{2-} (Fig. 1d2) have finer and smaller pore compared to S-Alg/P-Acc (Fig. 1b2). In cross-section view of Fig. 1b3-1b4, the images show that S-Alg/P-acc has smooth and compact structure with less pore visibility. In contrast, hydrogel beads with the presence of PO_4^{3-} (Fig. 2c3-2c4) and CO_3^{2-} (Fig. 2d3-2d4) have rather coarse surface and visible image of pore with porosity opening up to 12 μm in size, with filamentous formations inside the hollow spaces of the hydrogel beads. Clearly, the presence of anionic ions influences the structure of hydrogel beads.

Table 1 displays the percentage of porosity and the number of carboxyl groups in the hydrogel beads. Results show that the S-Alg/P-Acc@CO_3^{2-} and S-Alg/P-Acc@PO_4^{3-} composites had maximum porosities of 14.3 % and 10.9 %, respectively, while the S-Alg/P-Acc composite had a porosity of 9.5 %. The presence of anionic ions increased the porosity by 14.7–50.5 %, probably owing to the reinforcement of polymer networks resulting from the crosslinks between carboxylic acids bridged with calcium cations. The stiff polymer network retained the volume shrinkage of the beads during the drying process, maintaining a higher porosity. Meanwhile, the presence of anions may have led to a reduction in the carboxyl content of the S-Alg/P-Acc@CO_3^{2-} and S-Alg/P-Acc@PO_4^{3-} hydrogel beads because calcium ion capped some of the carboxyl groups, rendering them inactive for neutralization reactions. To confirm this hypothesis, the number of active carboxyl groups was quantitatively evaluated by titration method. The carboxyl groups possess a proton (H^+) that can be released by deprotonating the carboxyl group to form anions. This neutralization process decreases the concentration of carboxyl groups in the solution. Anions can be constituents of robust bases or other compounds that receive protons. For instance, the interaction between a carboxylic acid (RCOOH) and hydroxide ion (OH−).

$$\mathrm{RCOOH} + \mathrm{OH^-} \rightarrow \mathrm{RCOO^-} + \mathrm{H_2O} \tag{6}$$

During this chemical reaction, carboxylic acid (COOH) transfers its proton to the hydroxide ion (OH−), resulting in the formation of a carboxylate anion (RCOO−) and water (H_2O). This decreases the concentration of the COOH groups in the solution. As indicated in Table 1, the increased porosity of S-Alg/P-Acc@CO_3^{2-} led to a reduction in free carboxylic groups, supporting the molecular model suggesting that the polymer network is reinforced by the bridging of calcium ion between carboxyl groups.

Fig. 2 shows the FTIR spectra of the hydrogel beads. The peaks at 3362 cm^{-1}, 3364 cm^{-1} and 3365 cm^{-1} are ascribed to O–H stretching [32]. The absorption peaks at 1541 cm^{-1} from S-Alg/P-Acc decreased to 1539 cm^{-1} and 1538 cm^{-1} for S-Alg/P-Acc@PO_4^{3-} and S-Alg/P-Acc@CO_3^{2-}, respectively, possibly due to interaction of anionic ions with the -COO- groups in S-Alg and P-Acc. The bands detected around 1418 cm^{-1}, 1329 cm^{-1}, and 1026 cm^{-1} are due to symmetric-COO-, O–H bending vibrations, and C–O–C, respectively [14].

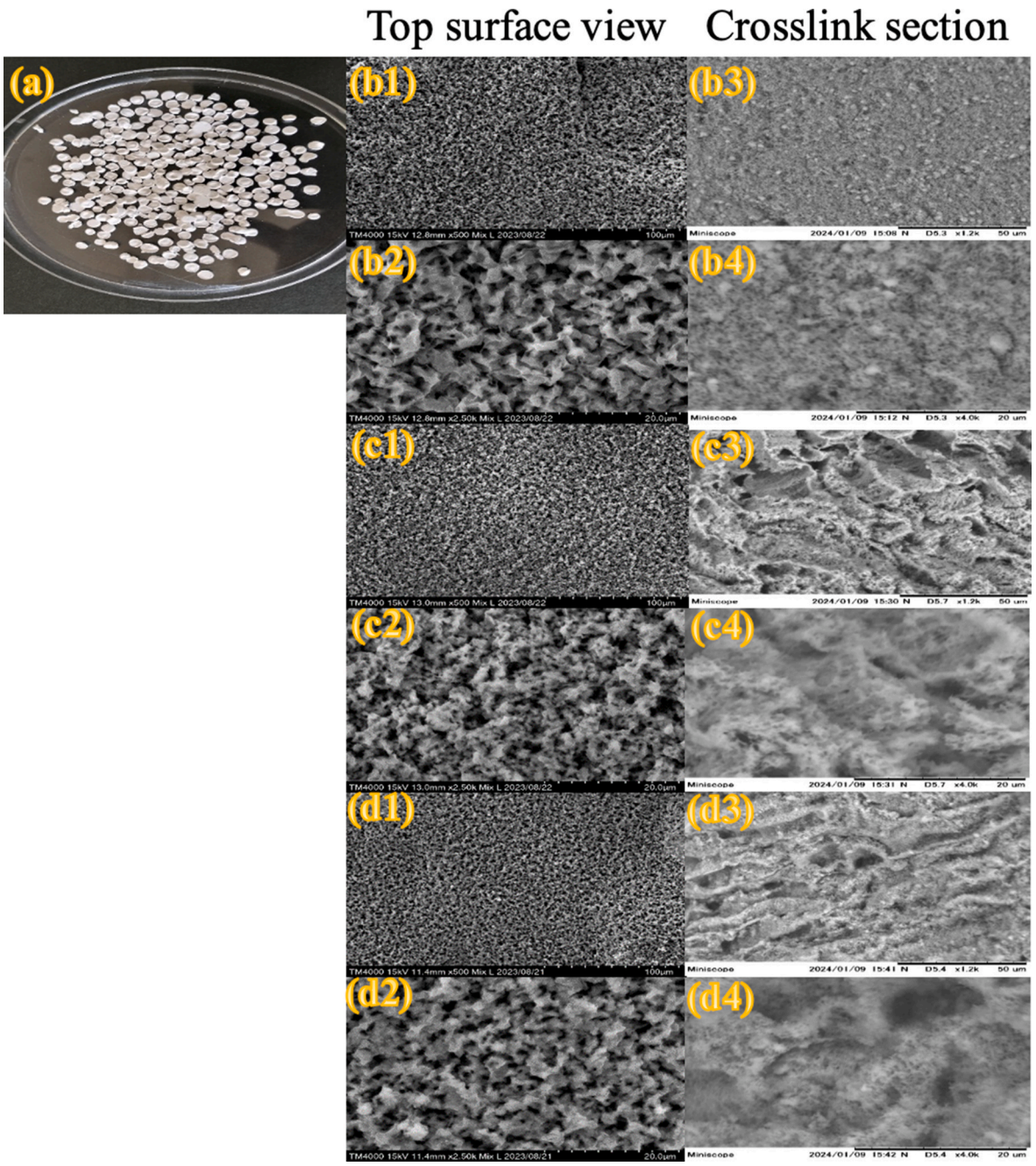

Fig. 1. (a) photograph of dried hydrogel beads. SEM images of morphology dried hydrogel beads (b1-b4) S-Alg/P-Acc (c1-c4) S-Alg/P-Acc@PO_4^{3-} (d1-d4) S-Alg/P-Acc@CO_3^{2-}.

3.2. *Swelling behaviour*

Hydrogel beads utilized for soil conditioner purposes must undergo water absorption during swelling [33]. In this step, water is absorbed without hindrance, resulting in the dissociation of the ionic groups, charged groups repulsion, and swelling of the polymer chains to create volumes filled with water molecules [34]. The primary aim was to analyze the swelling characteristics of the hydrogel beads at pH 4, 7, and 9 (Fig. 3). The swelling percentage of S-Alg/P-Acc was higher under acidic conditions (pH 4) than that of S-Alg/P-Acc@PO_4^{3-} and S-Alg/P-Acc@CO_3^{2-}, but lower under neutral and basic conditions. The lowest swelling percentage observed was a consequence of the protonation of the COOH groups, lead to the formation of COOH and a reduction in the repulsion between PO_4^{3-} and CO_3^{2-} anions. Simultaneously, this process strengthens the –OH-bonding contact between carboxylate groups, causing the shrinkage of the hydrogel [35,36].

The maximum swelling for S-Alg/P-Acc@CO_3^{2-} and S-Alg/P-Acc@PO_4^{3-} occurred at pH 7, likely due to steric hindrance or repulsion generated by the anions (CO_3^{2-} and PO_4^{3-}) near the hydrophobic part of the polymer chains. The hydrophobic portions of the hydrogel beads were transformed into hydrophilic elements through ionic effects, selectively interacting with nearby water molecules [3]. At a higher pH beyond 7 led to a reduction in the swelling percentage of S-Alg/P-Acc@PO_4^{3-} and S-Alg/P-Acc@CO_3^{2-}. This reaction may be due to the formation of a screening effect by the additional Na^+ cations, which shielded the charges on the COOH groups. Thus, the electrostatic repulsion between effective anions are weakened, leading to a decrease in water absorption [37].

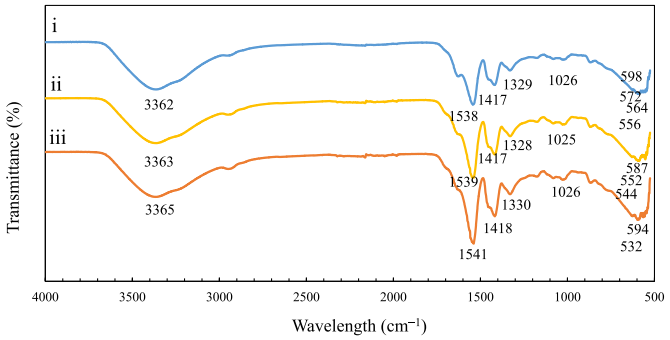

Fig. 2. FTIR spectra of hydrogel beads (i) S-Alg/P-Acc (ii) S-Alg/P-Acc@PO_4^{3-} (iii) S-Alg/P-Acc@CO_3^{2-}.

Table 1
Porosity percentage of hydrogel beads.

Samples	Porosity (%)	COOH (mmol/g)
S-Alg/P-Acc	9.54	25.87 ± 10.18
S-Alg/P-Acc@PO_4^{3-}	10.90	25.02 ± 14.83
S-Alg/P-Acc@CO_3^{2-}	14.31	3.23 ± 0.98

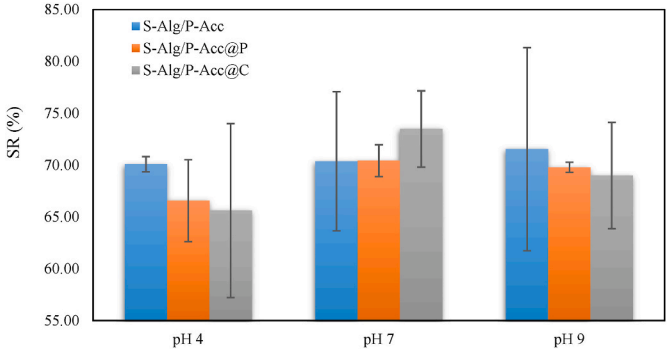

Fig. 3. Initial pH versus swelling properties of hydrogel beads.

3.3. Soil water loss studies

Fig. 4 shows the soil water loss (SWL) percentage over the 14-day period, including soils with hydrogel beads. The results indicated that S-Alg/P-Acc@PO_4^{3-} hydrogel beads exhibited great water retention capability and the lowest soil water loss, with a SWL value of 48 %. The SWLs of the S-Alg/P-Acc@CO_3^{2-} and S-Alg/P-Acc demonstrated values of 51 % and 49 %, respectively. In contrast, the SWL of soil was approximately 68 %.

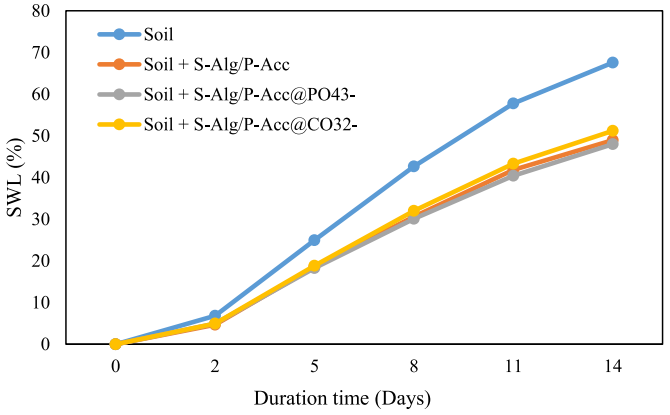

Fig. 4. Contact time effect of hydrogel beads versus soil water loss.

Initially, the incorporation of phosphate and carbonate ions into the hydrogel beads were expected to affect water retention via changing the distribution of pore sizes and improved the surface area and pore volume [38–40]. This can be proven by the percentage of porosity of the hydrogel beads as shown in Table 1. These ions normally can form multidirectional crosslinking with polyacrylic acid and lead to a better network flexibility and water storage capacity [41]. However, based on the graph shown in Fig. 4, the effect of phosphate and carbonate ions does not seem to be significant. Furthermore, hydrogel beads with the highest porosity percentage (Table 1) showed lower efficiency in water absorption under the investigated soil conditions. These phenomena could be caused by the density of the hydrogel beads and environmental factors, such as humidity and air temperature, which may have influenced the beads` water-holding capacity [27]. Importantly, all the soils containing the hydrogel beads had significantly reduced water loss in soil by approximately a 30 % smaller SWL compared to that of the intact soil.

3.4. Response of soil properties to hydrogel beads application

Figs. 5 and 6 demonstrated the effects of the hydrogel beads on the soil characteristics. The addition of hydrogel beads did not significantly impact the soil pH (Fig. 5a) and C/N ratio (Fig. 5b) (P-value <0.05). In contrast, there was a significant increase (P-value <0.05) in soil EC with the addition of hydrogel beads (Fig. 5c). The maximum EC of the soil was observed in the following order: S-Alg/P-Acc@CO_3^{2-} > S-Alg/P-Acc > S-Alg/P-Acc@PO_4^{3-}. The increase in soil EC is attributed to the release of salt ions as hydrogel beads react with soil water.

Phosphorus (P) is a crucial element of soil and plant growth and cannot be replaced by any other elements [42]. A significant increase (P-value <0.05) in available P (0.50 ± 0.03 mg/g) was confirmed by the use of hydrogel beads for S-Alg/P-Acc@PO_4^{3-}, whereas there was a reduction in the application of S-Alg/P-Acc and S-Alg/P-Acc@CO_3^{2-} compared to the intact soil (Fig. 5d). P is known to have low mobility because it tends to precipitate, adsorb, and convert into organic forms [43]. It is critical to consider the possible effects of nutrient leaching using hydrogel beads. In this study, the available P content was expected to decrease because of the adsorption of the hydrogel beads (S-Alg/-P-Acc and S-Alg/P-Acc@CO_3^{2-}) since the soil pH is approximately 5.5, causing P to be present in the form of $H_2PO_4^-$. Electrostatic interactions may possibly form between the negatively charged $H_2PO_4^-$ and the hydrogel beads. Fig. 5e shows that the use of hydrogel beads significantly increased soil CEC compared with the intact soil, as the hydrogel beads may contain –OH and –COOH functional groups, which have the potential to enhance soil CEC [44]. The application of hydrogel beads substantially enhanced SOC compared to the intact soil (P-value <0.05) (Fig. 5f). The SOC of the soil was the highest in the following order: S-Alg/P-Acc > S-Alg/P-Acc@PO_4^{3-} > S-Alg/P-Acc@CO_3^{2-}. This may imply that the hydrogel beads retained water and able to help to maintain soil moisture at an appropriate level which might indirectly boost microbial activity by altering oxygen penetration into the soil, contributing to organic matter degradation and organic carbon production [45]. Soil Fe availability decreased considerably (P-value <0.05) in the following order: control > S-Alg/P-Acc@PO_4^{3-} > S-Alg/-P-Acc@ CO_3^{2-} > S-Alg/P-Acc, with a reduction of up to 89.86 % (Fig. 5g). These findings suggest that hydrogel beads have a beneficial effect on Fe immobilization in soil.

Furthermore, the addition of hydrogel beads considerably enhanced the available N–NH_4^+ level in the soil (P-value <0.05) (Fig. 6a). S-Alg/P-Acc@PO_4^{3-} had the highest concentration after treatment, up to 89.16 % of the intact soil. This was followed by S-Alg/P-Acc@CO_3^{2-} (79.72 %) and S-Alg/P-Acc (67.92 %). Moreover, the hydrogel bead applications significantly decreased the content of N–NO_3^- in soils, and it decreased from 79.00 ± 1.41 mg/Kg (soil) to 4.30 ± 0.42 mg/Kg (S-Alg/P-Acc@CO_3^{2-}) (P-value <0.05) (Fig. 6b). It might be indicated that

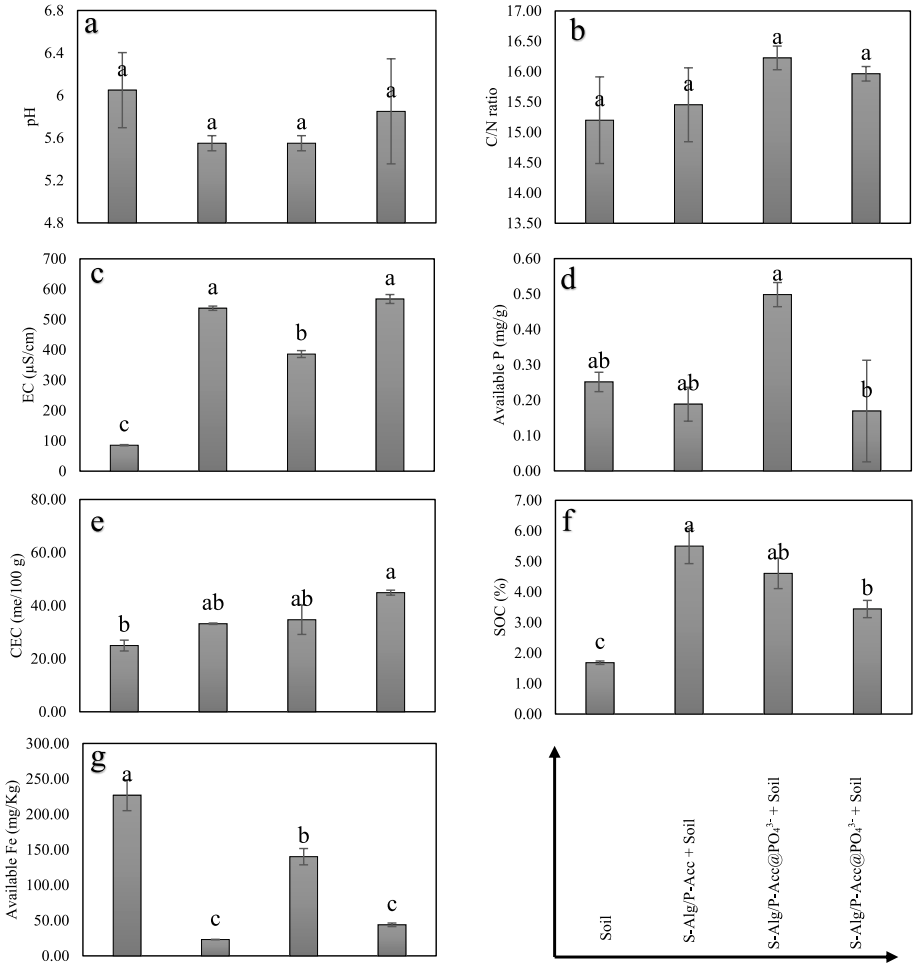

Fig. 5. Effect of hydrogel beads on soil pH, C/N ratio, electrical conductivity, available phosphorus, cation exchange capacity, soil organic carbon, and available Fe.

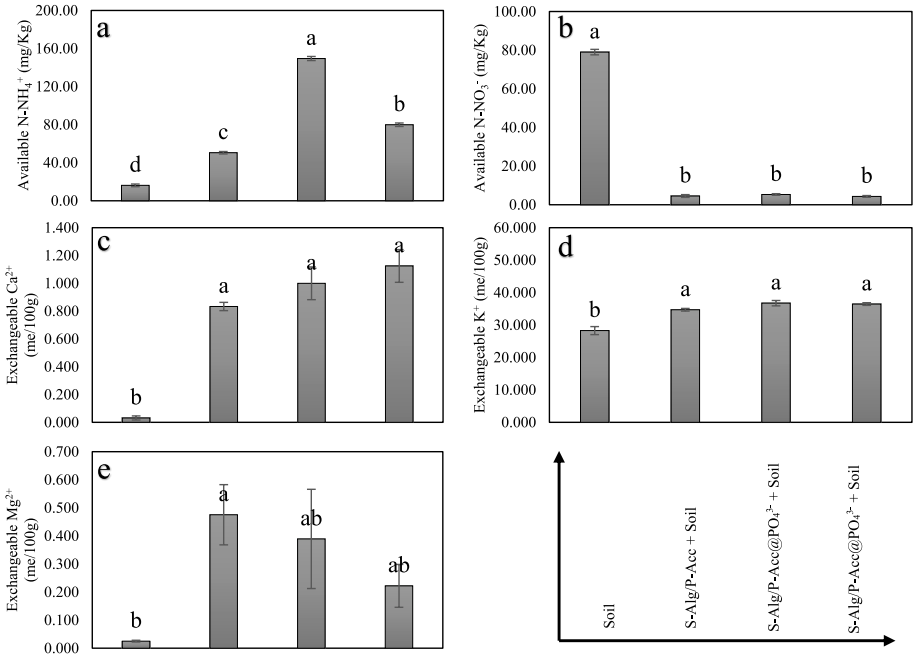

Fig. 6. Effect of hydrogel beads on soil available $N–NH_4^+$ and $N–NO_3^-$, and exchangeable Mg^{2+}, Ca^{2+} and K^+.

hydrogel beads application inhibit the transformation of N–NH_4^+ from oxidized into N–NO_3^- in soils. These results demonstrated similar trends with Zhang et al. [46] who used hydrogel-biochar composites for simultaneous enhancement and immobilization of nitrogen use and heavy metals, respectively. The hydrogel bead treatment resulted in considerably higher exchangeable Ca^{2+}, K^+, and Mg^{2+} levels compared to the intact soil (P-value <0.05) (Fig. 6c–e). Hydrogel beads may have the potential to absorb and retain water and assist in the transportation of ions in the soil, resulting in enhanced cations contents. It is interesting to note that exchangeable Mg^{2+} has a greater value for S-Alg/P-Acc compared to S-Alg/P-Acc@PO_4^{3-}, and S-Alg/P-Acc@CO_3^{2-}. This might indicated that the presence of PO_4^{3-} and CO_3^{2-} anionic ions from hydrogel beads may compete with Mg^{2+} ion for binding sites on soil particles through cation exchange process.

4. Conclusion

This study demonstrated the synthesis of hydrogel beads using sodium alginate (S-Alg) and poly (acrylic acid) (P-Acc) as the major components, with Ca^{2+} ions serving as an effective cross-linking agent. Hydrogel beads, both in the absence (S-Alg/P-Acc) and presence of PO_4^{3-} (S-Alg/P-Acc@PO_4^{3-}) and CO_3^{2-} (S-Alg/P-Acc@CO_3^{2-}) were examined in terms of swelling behavior, soil water loss (SWL), and soil properties. Hydrogel beads showed better water absorption properties and 30 % suppression of SWL capabilities compared with the control (intact soil). There were no significant changes in the soil pH and C/N ratio after the application of hydrogel beads. Nevertheless, the N–NH_4^+ concentration increased while N–NO_3^- decreased. Hydrogel bead treatment may hinder the conversion of N–NH_4^+ to N–NO_3^- via nitrification in soils. In addition, there was a simultaneous improvement in the levels of available phosphorus (P), cation exchange capacity (CEC), soil organic carbon (SOC), exchangeable cations (Ca^{2+}, K^+, and Mg^{2+}), and immobilization of Fe by up to 89.86 %. The presence of hydroxyl (-OH) and carboxyl (-COOH) groups is essential for improving soil characteristics and facilitating water retention.

CRediT authorship contribution statement

Endar Hidayat: Writing – review & editing, Writing – original draft, Visualization, Validation, Software, Methodology, Investigation, Formal analysis, Data curation, Conceptualization. **Nur Maisarah Mohamad Sarbani:** Writing – review & editing, Validation. **Sudip Kumar Lahiri:** Writing – review & editing. **Sadaki Samitsu:** Writing – review & editing, Validation, Supervision. **Seiichiro Yonemura:** Supervision. **Yoshiharu Mitoma:** Supervision. **Hiroyuki Harada:** Supervision, Project administration, Data curation.

Declaration of competing interest

The authors declare that they have no known competing financial interests or personal relationships that could have appeared to influence the work reported in this paper.

Data availability

The authors are unable or have chosen not to specify which data has been used.

Acknowledgment

E.H. wishes to express gratitude to the MEXT Scholarship for providing sponsorship during studies at the Prefectural University of Hiroshima. E. H. would like to express gratitude to NIMS, Japan, for accepting the research internship. This work was partly supported by JSPS KAKENHI Grant Number [21H02006].

References

[1] B. Tomadoni, M.F. Salcedo, A.Y. Mansilla, C.A. Casalongué, V.A. Alvarez, Macroporous alginate-based hydrogels to control soil substrate moisture: effect on lettuce plants under drought stress, Eur. Polym. J. 137 (2020), https://doi.org/10.1016/j.eurpolymj.2020.109953.

[2] K. Wantzen, J. Mol, Soil erosion from agriculture and mining: a threat to tropical stream ecosystems, Agriculture 3 (2013) 660–683, https://doi.org/10.3390/agriculture3040660.

[3] A. Bibi, S.U. Rehman, R. Faiz, T. Akhtar, M. Nawaz, S. Bibi, Effect of surfactants on swelling capacity and kinetics of alginate-chitosan/CNTs hydrogel, Mater. Res. Express 6 (2019), https://doi.org/10.1088/2053-1591/ab0697.

[4] R. Vundavalli, S. Vundavalli, M. Nakka, D.S. Rao, Biodegradable nano-hydrogels in agricultural farming - alternative source for water resources, Proc. Mater. Sci. 10 (2015) 548–554, https://doi.org/10.1016/j.mspro.2015.06.005.

[5] M. Mahinroosta, Z. Jomeh Farsangi, A. Allahverdi, Z. Shakoori, Hydrogels as intelligent materials: a brief review of synthesis, properties and applications, Mater. Today Chem. 8 (2018) 42–55, https://doi.org/10.1016/j.mtchem.2018.02.004.

[6] A. Reghioua, D. Barkat, A.H. Jawad, A.S. Abdulhameed, S. Rangabhashiyam, M. R. Khan, Z.A. Alothman, Magnetic chitosan-glutaraldehyde/Zinc Oxide/Fe3O4 nanocomposite: optimization and adsorptive mechanism of remazol brilliant blue R dye removal, J. Polym. Environ. 29 (2021) 3932–3947, https://doi.org/10.1007/s10924-021-02160-z.

[7] R. El Kaim Billah, H. Lgaz, D.G. Jiménez, P. Pal, B. Trujillo-Navarrete, M. Ahrouch, J.S. Algethami, Y. Abdellaoui, H. Majdoubi, A.A. Alrashdi, M. Agunaou, A. Soufiane, E.A. López-Maldonado, Experimental and Theoretical Studies on Nitrate Removal Using Epichlorohydrin-Modified Cross-Linked Chitosan Derived from Shrimp Waste, Environmental Science and Pollution Research, 2023, https://doi.org/10.1007/s11356-023-29896-6.

[8] T. Jóźwiak, U. Filipkowska, P. Szymczyk, J. Rodziewicz, A. Mielcarek, Effect of ionic and covalent crosslinking agents on properties of chitosan beads and sorption effectiveness of Reactive Black 5 dye, React. Funct. Polym. 114 (2017) 58–74, https://doi.org/10.1016/j.reactfunctpolym.2017.03.007.

[9] S. Zhang, X. Fan, F. Zhang, Y. Zhu, J. Chen, Synthesis of emulsion-templated magnetic porous hydrogel beads and their application for catalyst of fenton reaction, Langmuir 34 (2018) 3669–3677, https://doi.org/10.1021/acs.langmuir.8b00009.

[10] S. Zhang, Y. Zhang, L. Fu, M. Jing, A chitosan fiber as green material for removing Cr(VI) ions and Cu(II) ions pollutants, Sci. Rep. 11 (2021), https://doi.org/10.1038/s41598-021-02399-5.

[11] I. Kassem, Z. Kassab, M. Khouloud, H. Sehaqui, R. Bouhfid, J. Jacquemin, A.E. K. Qaiss, M. El Achaby, Phosphoric acid-mediated green preparation of regenerated cellulose spheres and their use for all-cellulose cross-linked superabsorbent hydrogels, Int. J. Biol. Macromol. 162 (2020) 136–149, https://doi.org/10.1016/j.ijbiomac.2020.06.136.

[12] E. Caló, V.V. Khutoryanskiy, Biomedical applications of hydrogels: a review of patents and commercial products, Eur. Polym. J. 65 (2015) 252–267, https://doi.org/10.1016/j.eurpolymj.2014.11.024.

[13] Z. Tariq, D.N. Iqbal, M. Rizwan, M. Ahmad, M. Faheem, M. Ahmed, Significance of biopolymer-based hydrogels and their applications in agriculture: a review in perspective of synthesis and their degree of swelling for water holding, RSC Adv. 13 (2023) 24731–24754, https://doi.org/10.1039/D3RA03472K.

[14] S. Hua, H. Ma, X. Li, H. Yang, A. Wang, pH-sensitive sodium alginate/poly(vinyl alcohol) hydrogel beads prepared by combined Ca2+ crosslinking and freeze-thawing cycles for controlled release of diclofenac sodium, Int. J. Biol. Macromol. 46 (2010) 517–523, https://doi.org/10.1016/j.ijbiomac.2010.03.004.

[15] E. Baigorria, L.A. Cano, L.M. Sanchez, V.A. Alvarez, R.P. Ollier, Bentonite-composite polyvinyl alcohol/alginate hydrogel beads: preparation, characterization and their use as arsenic removal devices, Environ. Nanotechnol. Monit. Manag. 14 (2020), https://doi.org/10.1016/j.enmm.2020.100364.

[16] W. Li, L. Zhang, D. Hu, R. Yang, J. Zhang, Y. Guan, F. Lv, H. Gao, A mesoporous nanocellulose/sodium alginate/carboxymethyl-chitosan gel beads for efficient adsorption of Cu2+ and Pb2+, Int. J. Biol. Macromol. 187 (2021) 922–930, https://doi.org/10.1016/j.ijbiomac.2021.07.181.

[17] S. Tang, Y. Zhao, H. Wang, Y. Wang, H. Zhu, Y. Chen, S. Chen, S. Jin, Z. Yang, P. Li, S. Li, Preparation of the sodium alginate-g-(polyacrylic acid-co-allyltrimethylammonium chloride) polyampholytic superabsorbent polymer and its dye adsorption property, Mar. Drugs 16 (2018), https://doi.org/10.3390/md16120476.

[18] F. Meng, S. Zhang, Y. Oh, Z. Zhou, H.S. Shin, S.R. Chae, Fouling in membrane bioreactors: an updated review, Water Res. 114 (2017) 151–180, https://doi.org/10.1016/j.watres.2017.02.006.

[19] M. Eshwar, M. Srilatha, K.B. Rekha, S.H.K. Sharma, Characterization of humic substances by functional groups and spectroscopic methods, Int. J. Curr. Microbiol. Appl. Sci. 6 (2017) 1768–1774, https://doi.org/10.20546/ijcmas.2017.610.213.

[20] L. Curti, O.W. Moore, P. Babakhani, K.Q. Xiao, C. Woulds, A.W. Bray, B.J. Fisher, M. Kazemian, B. Kaulich, C.L. Peacock, Carboxyl-richness controls organic carbon preservation during coprecipitation with iron (oxyhydr)oxides in the natural environment, Commun. Earth Environ. 2 (2021), https://doi.org/10.1038/s43247-021-00301-9.

[21] S. Jezierska-Tys, S. Wesołowska, A. Gałązka, J. Joniec, J. Bednarz, R. Cierpiała, Biological activity and functional diversity in soil in different cultivation systems, Int. J. Environ. Sci. Technol. 17 (2020) 4189–4204, https://doi.org/10.1007/s13762-020-02762-5.

[22] N. Sheikh, L. Jalili, F. Anvari, A study on the swelling behavior of poly(acrylic acid) hydrogels obtained by electron beam crosslinking, Radiat. Phys. Chem. 79 (2010) 735–739, https://doi.org/10.1016/j.radphyschem.2009.12.013.
[23] R. Faturechi, A. Karimi, A. Hashemi, H. Yousefi, M. Navidbakhsh, Influence of Poly (acrylic acid) on the mechanical properties of composite hydrogels, Adv. Polym. Technol. 34 (2015), https://doi.org/10.1002/adv.21487.
[24] K. Murai, Y. Funamizu, T. Ogura, K. Nishio, Bioinspired mineralization of calcium carbonate in peptide hydrogel acting as a multifunctional three-dimensional template, J. Asian Ceram. Soc. 9 (2021) 771–781, https://doi.org/10.1080/21870764.2021.1911060.
[25] S. Sornkamnerd, M.K. Okajima, T. Kaneko, Tough and porous hydrogels prepared by simple lyophilization of LC gels, ACS Omega 2 (2017) 5304–5314, https://doi.org/10.1021/acsomega.7b00602.
[26] H. Yang, A. Tejado, N. Alam, M. Antal, T.G.M. van de Ven, Films prepared from electrosterically stabilized nanocrystalline cellulose, Langmuir 28 (2012) 7834–7842, https://doi.org/10.1021/la2049663.
[27] N.E. Rabat, S. Hashim, R.A. Majid, Effect of different monomers on water retention properties of slow release fertilizer hydrogel, in: Procedia Eng, Elsevier Ltd, 2016, pp. 201–207, https://doi.org/10.1016/j.proeng.2016.06.573.
[28] E. Hidayat, A. Afriliana, G. Gusmini, M. Taizo, H. Harada, Evaluate of coffee husk compost, Int. J. Food, Agric. Nat. Resour. 1 (2020) 37–43, https://doi.org/10.46676/ij-fanres.v1i1.8.
[29] M. Iatrou, A. Papadopoulos, F. Papadopoulos, O. Dichala, P. Psoma, A. Bountla, Determination of soil available phosphorus using the olsen and mehlich 3 methods for Greek soils having variable amounts of calcium carbonate, Commun. Soil Sci. Plant Anal. 45 (2014) 2207–2214, https://doi.org/10.1080/00103624.2014.911304.
[30] E. Hidayat, H. Harada, Simultaneously recovery of phosphorus and potassium using bubble column reactor as struvite-K and implementation on crop growth, in: Crystallization and Applications, IntechOpen, 2022, https://doi.org/10.5772/intechopen.100103.
[31] H. Xi, M. Jia, Y. Kuzyakov, Z. Peng, Y. Zhang, J. Han, G. Ali, L. Mao, J. Zhang, T. Fan, Y. Liu, Key decomposers of straw depending on tillage and fertilization, Agric. Ecosyst. Environ. 358 (2023) 108717, https://doi.org/10.1016/j.agee.2023.108717.
[32] D. Das, S. Bhattacharjee, S. Bhaladhare, Preparation of cellulose hydrogels and hydrogel nanocomposites reinforced by crystalline cellulose nanofibers (CNFs) as a water reservoir for agriculture use, ACS Appl. Polym. Mater. 5 (2023) 2895–2904, https://doi.org/10.1021/acsapm.3c00109.
[33] A. Di Martino, Y.A. Khan, S. Durpekova, V. Sedlarik, O. Elich, J. Cechmankova, Ecofriendly renewable hydrogels based on whey protein and for slow release of fertilizers and soil conditioning, J. Clean. Prod. 285 (2021), https://doi.org/10.1016/j.jclepro.2020.124848.
[34] C.G. Kees de Kruif, S.G. Anema, C. Zhu, P. Havea, C. Coker, Water holding capacity and swelling of casein hydrogels, Food Hydrocolloids 44 (2015) 372–379, https://doi.org/10.1016/j.foodhyd.2014.10.007.
[35] S.M. Lohmousavi, H.H.S. Abad, G. Noormohammadi, B. Delkhosh, Synthesis and characterization of a novel controlled release nitrogen-phosphorus fertilizer hybrid nanocomposite based on banana peel cellulose and layered double hydroxides nanosheets, Arab. J. Chem. 13 (2020) 6977–6985, https://doi.org/10.1016/j.arabjc.2020.06.042.
[36] U.R. Tulain, M. Ahmad, A. Rashid, M.Z. Malik, F.M. Iqbal, Fabrication of pH-responsive hydrogel and its in vitro and in vivo evaluation, Adv. Polym. Technol. 37 (2018) 290–304, https://doi.org/10.1002/adv.21668.
[37] W.-F. Lee, G.-H. Lin, Superabsorbent Polymeric Materials VIII: Swelling Behavior of Crosslinked Poly[Sodium Acrylate-Co-Trimethyl Methacryloyloxyethyl Ammonium Iodide] in Aqueous Salt Solutions, 2000.
[38] F. Han, S. An, L. Liu, L. Ma, Y. Wang, L. Yang, Simultaneous enhancement of soil properties along with water-holding and restriction of Pb–Cd mobility in a soil-plant system by the addition of a phosphorus-modified biochar to the soil, J. Environ. Manag. 345 (2023) 118827, https://doi.org/10.1016/j.jenvman.2023.118827.
[39] H. Liu, J. Zhang, N. Bao, C. Cheng, L. Ren, C. Zhang, Textural properties and surface chemistry of lotus stalk-derived activated carbons prepared using different phosphorus oxyacids: adsorption of trimethoprim, J. Hazard Mater. 235–236 (2012) 367–375, https://doi.org/10.1016/j.jhazmat.2012.08.015.
[40] Y. Chen, Y. Gao, C.W.W. Ng, H. Guo, Bio-improved hydraulic properties of sand treated by soybean urease induced carbonate precipitation and its application Part 1: water retention ability, Transport. Geotechn. 27 (2021) 100489, https://doi.org/10.1016/j.trgeo.2020.100489.
[41] Y. Jiao, T. Su, Y. Chen, M. Long, X. Luo, X. Xie, Z. Qin, Enhanced water absorbency and water retention rate for superabsorbent polymer via porous calcium carbonate crosslinking, Nanomaterials 13 (2023) 2575, https://doi.org/10.3390/nano13182575.
[42] T.S.S. Neset, D. Cordell, Global phosphorus scarcity: identifying synergies for a sustainable future, J. Sci. Food Agric. 92 (2012) 2–6, https://doi.org/10.1002/jsfa.4650.
[43] M. Dixon, E. Simonne, T. Obreza, G. Liu, Crop response to low phosphorus bioavailability with a focus on tomato, Agronomy 10 (2020) 617, https://doi.org/10.3390/agronomy10050617.
[44] L. van Zwieten, S. Kimber, S. Morris, K.Y. Chan, A. Downie, J. Rust, S. Joseph, A. Cowie, Effects of biochar from slow pyrolysis of papermill waste on agronomic performance and soil fertility, Plant Soil 327 (2010) 235–246, https://doi.org/10.1007/s11104-009-0050-x.
[45] W. Zhou, D. Hui, W. Shen, Effects of soil moisture on the temperature sensitivity of soil heterotrophic respiration: a laboratory incubation study, PLoS One 9 (2014) e92531, https://doi.org/10.1371/journal.pone.0092531.
[46] L. Zhang, Y. Guan, Microbial investigations of new hydrogel-biochar composites as soil amendments for simultaneous nitrogen-use improvement and heavy metal immobilization, J. Hazard Mater. 424 (2022), https://doi.org/10.1016/j.jhazmat.2021.127154.